

# Evection resonance in the hierarchical restricted 3-body problem

Songnan QI

Supervisor: Jérémie COUTURIER

Co-supervisor: Adrien LELEU

January 13, 2025



**UNIVERSITÉ  
DE GENÈVE**

**FACULTY OF SCIENCE**

Department of Astronomy

# Contents

<b>1</b>	<b>Introduction</b>	<b>1</b>
<b>2</b>	<b>Analytical model</b>	<b>2</b>
2.1	Hamiltonian computations . . . . .	2
2.1.1	Three-degree-of-freedom Hamiltonian . . . . .	2
2.1.2	One-degree-of-freedom Hamiltonian . . . . .	3
2.1.3	Autonomous one-parameter dimensionless Hamiltonian . . . . .	6
2.2	Analysis of the phase space $H(\Phi; \phi)$ . . . . .	10
2.2.1	Bifurcations of topology of the phase space . . . . .	10
2.2.2	History of the parameter $\delta$ and the two ejection resonances . . . . .	12
<b>3</b>	<b>Numerical simulations</b>	<b>14</b>
3.1	Simulation for the Sun-Earth-Moon system . . . . .	14
3.1.1	Searching for the second ejection resonance in the future . . . . .	15
3.1.2	Searching for the first ejection resonance in the past . . . . .	15
3.2	Simulation for the exoplanetary system of TOI-6303 b . . . . .	17
3.2.1	Selection of the planet . . . . .	17
3.2.2	Searching for second ejection resonance . . . . .	18
<b>4</b>	<b>Conclusion</b>	<b>19</b>
<b>5</b>	<b>Appendix</b>	<b>21</b>
5.1	Appendix A: Canonicity of the Poincaré variables . . . . .	21
5.2	Appendix B: Canonicity of the transformation $(\Phi, \phi) \rightarrow (X, Y)$ . . . . .	21



## 1 Introduction

The 3-body problem, whose goal is to study the trajectories of three bodies under their mutual gravity, has aroused a lot of interest since Isaac Newton published the famous book *The Mathematical Principles of Natural Philosophy*. Up to now, no general closed-form solution has been found for the general 3-body problem; however, it is still useful to work on simplified problems to comprehend the dynamics of celestial bodies, one of which is the hierarchical restricted 3-body problem. *restricted* means that one of the bodies is assumed to be infinitely massless compared to the others, whereas *hierarchical* means that the massless body is much closer to one body than the other, which then acts as a perturbation.

The goal of this project is to study the evaporation resonance in the hierarchical restricted 3-body problem, via both analytical and numerical approaches. The evaporation resonance is a second-order resonance between the mean longitude of the star  $\lambda_0$  and the longitude of periapsis of the satellite  $\varpi$ , as shown in the schema 1. It occurs when these two angles precess roughly at the same frequency, that is, when the periapsis of the particle follows the position of the perturbator. In this problem, I am particularly interested in the motion of the particle. To simplify the problem mathematically, small eccentricities and coplanar orbits are assumed.

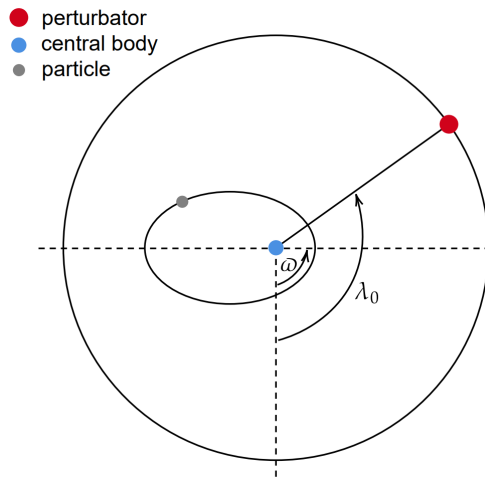


Figure 1: Schema of the hierarchical restricted 3-body problem

In the celestial mechanics context, any star-planet-satellite system, for instance the Sun-Earth-Moon system, is a hierarchical restricted 3-body system, where the star is the perturbator, the planet is the central body and the satellite is the particle.

In the analytical work, I'll derive the Hamiltonian of the particle and simplify it to an one-degree-of-freedom and one-parameter autonomous one. The evaporation resonance will appear as a change of topology in the phase space as the parameter varies. The last step is to confirm the existence of the evaporation resonance via numerical simulations, run with the N-body software NcorpiON [1], and to verify that it occurs where it's predicted to be.



## 2 Analytical model

### 2.1 Hamiltonian computations

#### 2.1.1 Three-degree-of-freedom Hamiltonian

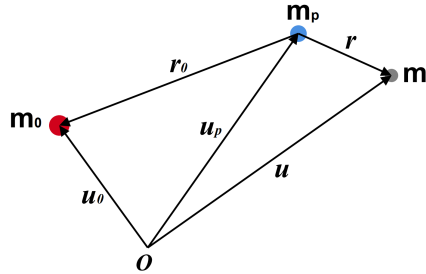


Figure 2: The three bodies in a reference frame with the origin point  $O$

To find the Hamiltonian of the problem, I start with the equations of motion of the three bodies, with the subscript "0" for the star, "p" for the planet and no subscript for the massless satellite.

$$\begin{cases} \ddot{\mathbf{u}} = -\frac{Gm_0(\mathbf{u} - \mathbf{u}_0)}{|\mathbf{u} - \mathbf{u}_0|^3} - \frac{Gm_p(\mathbf{u} - \mathbf{u}_p)}{|\mathbf{u} - \mathbf{u}_p|^3} \\ \ddot{\mathbf{u}}_0 = -\frac{Gm_p(\mathbf{u}_0 - \mathbf{u}_p)}{|\mathbf{u}_0 - \mathbf{u}_p|^3} \\ \ddot{\mathbf{u}}_p = -\frac{Gm_p(\mathbf{u}_p - \mathbf{u}_0)}{|\mathbf{u}_p - \mathbf{u}_0|^3} \end{cases} \quad (1)$$

Since only the relative positions are important, the equations of motion can be transformed by defining  $\mathbf{r} = \mathbf{u} - \mathbf{u}_p$ ,  $\mathbf{r}_0 = \mathbf{u}_0 - \mathbf{u}_p$ .

$$\begin{cases} \ddot{\mathbf{r}} = -Gm_0 \left( \frac{\mathbf{r}_0}{r_0^3} + \frac{\mathbf{r} - \mathbf{r}_0}{|\mathbf{r} - \mathbf{r}_0|^3} \right) - Gm_p \frac{\mathbf{r}}{r^3} \\ \ddot{\mathbf{r}}_0 = -G(m_0 + m_p) \frac{\mathbf{r}_0}{r_0^3} \end{cases} \quad (2)$$

The Hamiltonian of a massless particle is given by

$$H = \mathbf{v} \cdot \dot{\mathbf{r}} - \mathcal{L} \quad (3)$$

such that

$$\begin{cases} \dot{\mathbf{r}} = \frac{\partial H}{\partial \mathbf{v}} \\ \dot{\mathbf{v}} = -\frac{\partial H}{\partial \mathbf{r}} \end{cases} \quad (4)$$

where  $\mathbf{v} = d\mathbf{r}/dt$ , and the Lagrangian is defined as  $\mathcal{L} = (E_k - E_p)/m$ .



Combining together the equations 2 and 3, I obtain

$$\begin{aligned}
 H = (\mathbf{v} \cdot \dot{\mathbf{r}} - \mathcal{L}) &= \dot{r}^2 - \left( \frac{1}{2} \dot{r}^2 - \int_{\mathcal{C}} -\ddot{\mathbf{r}}' d\mathbf{r}' \right) \\
 &= \frac{1}{2} \dot{r}^2 + \int_{\mathcal{C}} -\ddot{\mathbf{r}}' d\mathbf{r}' \\
 &= \left( \frac{1}{2} \dot{r}^2 - \frac{Gm_p}{r} \right) + Gm_0 \left( \frac{\mathbf{r}_0 \cdot \mathbf{r}}{r_0^3} - \frac{1}{|\mathbf{r} - \mathbf{r}_0|} \right) \\
 &= H_K + H_P
 \end{aligned} \tag{5}$$

where  $\mathcal{C}$  is the trajectory taken from infinity to its position in the reference frame where the planet  $m_p$  is at the origin.

The Hamiltonian is made up of two parts:

- The keplerian part simplified by the Vis-viva equation with  $a$  defined as the semi-major axes of the particles's orbit:

$$H_K = \frac{1}{2} \dot{r}^2 - \frac{Gm_p}{r} = \frac{1}{2} Gm_p \left( \frac{2}{r} - \frac{1}{a} \right) - \frac{Gm_p}{r} = -\frac{Gm_p}{2a} \tag{6}$$

- The perturbative part simplified due to the hierarchy of the problem  $r/r_0 \ll 1$ :  
By expanding  $1/|\mathbf{r} - \mathbf{r}_0|$  to the 2<sup>nd</sup> order, I get

$$\begin{aligned}
 \frac{1}{|\mathbf{r} - \mathbf{r}_0|} &= \frac{1}{r_0} \left( 1 - \frac{2\mathbf{r} \cdot \mathbf{r}_0}{r_0^2} + \frac{r^2}{r_0^2} \right)^{-\frac{1}{2}} \\
 &= \frac{1}{r_0} \left( 1 + \frac{\mathbf{r} \cdot \mathbf{r}_0}{r_0^2} - \frac{1}{2} \frac{r^2}{r_0^2} + \frac{3}{2} \frac{(\mathbf{r} \cdot \mathbf{r}_0)^2}{r_0^4} + \mathcal{O}\left(\frac{r^3}{r_0^3}\right) \right)
 \end{aligned} \tag{7}$$

as well as the perturbative part of the Hamiltonian

$$H_P = Gm_0 \left( -\frac{1}{r_0} + \frac{1}{2} \frac{r^2}{r_0^3} - \frac{3}{2} \frac{(\mathbf{r}_0 \cdot \mathbf{r})^2}{r_0^5} \right) \tag{8}$$

Notice that the term of first order is canceled out by  $Gm_0(\mathbf{r}_0 \cdot \mathbf{r})/r_0^3$  in the perturbative part. If  $1/|\mathbf{r} - \mathbf{r}_0|$  is only expanded to the first order, the perturbative Hamiltonian will disappear completely. Since the constant  $-Gm_0/r_0$  can be removed from the Hamiltonian without changing the solutions, the three-degree-of-freedom Hamiltonian  $H(\mathbf{r}; \dot{\mathbf{r}})$  can be written as

$$H = -\frac{Gm_p}{2a} + Gm_0 \left( \frac{1}{2} \frac{r^2}{r_0^3} - \frac{3}{2} \frac{(\mathbf{r}_0 \cdot \mathbf{r})^2}{r_0^5} \right) \tag{9}$$

with the Hamilton's equations given by equations 4.

### 2.1.2 One-degree-of-freedom Hamiltonian

Since I only care about the orbit itself rather than the position of the satellite on its orbit, I average the Hamiltonian over the mean anomaly to remove the information about



the latter [2, 3]. From the Kepler's equation  $M = E - e \sin E$ , I get  $dM = (r/a)dE$  [2]. Therefore the averaged Hamiltonian becomes

$$\bar{H} = \frac{1}{T} \int_0^T H dt = \frac{1}{2\pi} \int_0^{2\pi} H dM = -\frac{Gm_p}{2a} + Gm_0 \left( \frac{1}{2} \frac{\bar{r}^2}{r_0^3} - \frac{3}{2} \frac{\overline{(\mathbf{r}_0 \cdot \mathbf{r})^2}}{r_0^5} \right) \quad (10)$$

The averaged quantities in the equation above are defined by

$$\begin{aligned} \bar{r}^2 &= \frac{1}{T} \int_0^T r^2 dt \\ \overline{(\mathbf{r}_0 \cdot \mathbf{r})^2} &= \frac{1}{T} \int_0^T (\mathbf{r}_0 \cdot \mathbf{r})^2 dt \end{aligned} \quad (11)$$

Assuming that  $(\hat{\mathbf{i}}, \hat{\mathbf{j}}, \hat{\mathbf{k}})$  is the frame basis for the particle's orbit and  $(\hat{\mathbf{I}}, \hat{\mathbf{J}}, \hat{\mathbf{K}})$  for the orbit of the perturbator around the origin  $m_p$ . Assuming also that both orbits are in the same plane  $\hat{\mathbf{k}}/\hat{\mathbf{K}}$ , I get the expressions for the averaged quantities  $\bar{r}^2$  and  $\overline{(\mathbf{r}_0 \cdot \mathbf{r})^2}$ :

$$\begin{aligned} \bar{r}^2 &= \frac{1}{2\pi} \int_0^{2\pi} r^2 \frac{r}{a} dE = \frac{1}{2\pi} \int_0^{2\pi} a^2 (1 - e \cos E)^3 dE = a^2 \left( \frac{3}{2} e^2 + 1 \right) \\ \overline{(\mathbf{r}_0 \cdot \mathbf{r})^2} &= {}^t \mathbf{r}_0 (\mathbf{r} \cdot {}^t \mathbf{r}) \mathbf{r}_0 \\ &= {}^t \mathbf{r}_0 \cdot \left[ \frac{1}{2\pi} \int_0^{2\pi} \begin{pmatrix} x^2 & xy & 0 \\ xy & y^2 & 0 \\ 0 & 0 & 0 \end{pmatrix} \frac{r}{a} dE \right] \mathbf{r}_0 = {}^t \mathbf{r}_0 \cdot \frac{a^2}{2} \begin{pmatrix} 4e^2 + 1 & 0 & 0 \\ 0 & 1 - e^2 & 0 \\ 0 & 0 & 0 \end{pmatrix} \mathbf{r}_0 \quad (12) \\ &= {}^t \mathbf{r}_0 \cdot \frac{a^2}{2} [(1 - e^2)(\mathbb{I} - \hat{\mathbf{k}}^t \hat{\mathbf{k}}) + 5e^2 \hat{\mathbf{i}}^t \hat{\mathbf{i}}] \cdot \mathbf{r}_0 \\ &= \frac{a^2}{2} \left( (1 - e^2) [r_0^2 - (\hat{\mathbf{k}} \cdot \mathbf{r}_0)^2] + 5e^2 (\hat{\mathbf{i}} \cdot \mathbf{r}_0)^2 \right) \end{aligned}$$

where  $\mathbb{I}$  is an identity matrix of 3x3, and the transpose of a matrix  $\mathcal{M}$  is denoted by  ${}^t \mathcal{M}$ .

I then transform the averaged Hamiltonian from Cartesian coordinates  $(\mathbf{r}; \dot{\mathbf{r}})$  to elliptic elements  $(a, e, i; M, \omega, \Omega)$ , knowing the relations between them [2]

$$\begin{cases} x = r \cos \nu = a(\cos E - e) \\ y = r \sin \nu = a\sqrt{1 - e^2} \sin E \\ r = a(1 - e \cos E) \end{cases} \quad (13)$$

where

- $M = nt = \frac{2\pi}{T}t$ : the mean anomaly of the particle, defined by the mean swept angle at time t;
- $\omega$ : the argument of periapsis, which is the angle from the ascending node to its periapsis;
- $\Omega$ : the longitude of ascending node, which is the angle from a direction of reference to the ascending node;
- $\nu$  the true anomaly and  $E$  the eccentric anomaly, as shown in the figure 3.

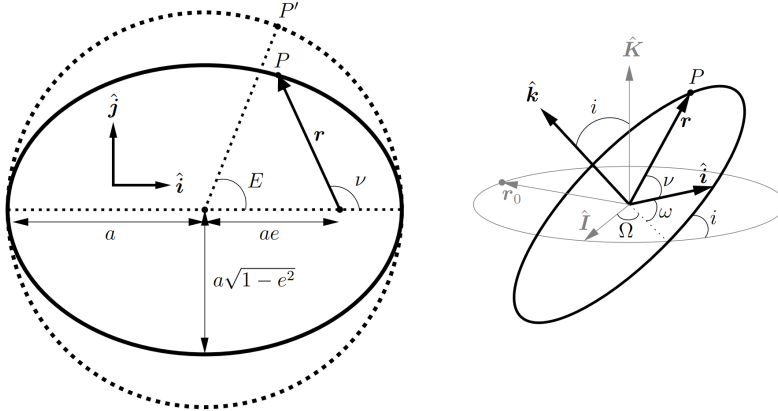


Figure 3: The elliptic elements [4]

With the gravitational parameter  $\mu = Gm_p$ , the averaged Hamiltonian in elliptic coordinates is

$$\bar{H} = -\left(\frac{\mu}{2a} - \frac{Gm_0a^2}{4r_0^3}\right) + \frac{3Gm_0a^2e^2}{2r_0^3} + \frac{3Gm_0a^2}{4r_0^5} \left[ (1-e^2) (\hat{k} \cdot \mathbf{r}_0)^2 - 5e^2 (\hat{i} \cdot \mathbf{r}_0)^2 \right] \quad (14)$$

However, the transformation from Cartesian coordinates to elliptic coordinates is not canonical, which means that the form of Hamilton's equations is not preserved. For a system of  $N$  degrees of freedom, a transformation is said to be canonical if there exists a  $N \times N$  non degenerate matrix  $\mathcal{A}$  and a function  $\Psi : \mathbb{R}^{2N} \rightarrow \mathbb{R}^{2N}$  that is linear and takes the form [5]:

$$\Psi : \begin{pmatrix} \mathbf{p} \\ \mathbf{q} \end{pmatrix} \mapsto \begin{pmatrix} \mathcal{A} & 0 \\ 0 & {}^t \mathcal{A}^{-1} \end{pmatrix} \begin{pmatrix} \mathbf{p} \\ \mathbf{q} \end{pmatrix} \quad (15)$$

In order to rewrite the Hamiltonian with canonical variables, I refer to the Delaunay variables as well as the Poincaré variables [3].

Delaunay variables  $(\Lambda, G, H; M, \omega, \Omega)$  with definitions

$$\begin{array}{l|l} \Lambda = \sqrt{\mu a} & M \\ G = \Lambda \sqrt{(1-e^2)} & \omega \\ H = G \cos i & \Omega \end{array}$$

are proved to be canonical by Laskar, 2017 [6].

The canonicity of the Poincaré variables  $(\Lambda, D, Z; \lambda, -\varpi, -\Omega)$  with

$$\begin{array}{l|l} \Lambda = \sqrt{\mu a} & \lambda = M + \varpi \\ D = \Lambda - G = \Lambda(1 - \sqrt{1-e^2}) & -\varpi = -\omega - \Omega \\ Z = G - H = G(1 - \cos i) & -\Omega \end{array}$$

are given in the Appendix A.



With the coplanar assumption,  $\hat{\mathbf{k}} \cdot \mathbf{r}_0 = \hat{\mathbf{K}} \cdot \mathbf{r}_0 = 0$ , I obtain the relations

$$\begin{cases} \mathbf{r}_0 = a_0(\cos \lambda_0 \hat{\mathbf{I}} + \sin \lambda_0 \hat{\mathbf{J}}) \\ \hat{\mathbf{i}} = \cos \varpi \hat{\mathbf{I}} + \sin \varpi \hat{\mathbf{J}} \end{cases} \Rightarrow \hat{\mathbf{i}} \cdot \mathbf{r}_0 = a_0 \cos(\lambda_0 - \varpi) \quad (16)$$

One degree of freedom is directly removed since the inclination is assumed to be 0. Assuming the orbit of the particle is circular,  $r_0 = a_0$ , I get

$$\begin{aligned} H(\Lambda, D; \lambda, -\varpi) &= -\left(\frac{\mu}{2a} - \frac{Gm_0 a^2}{4r_0^3}\right) + \frac{3Gm_0}{4r_0^3} a^2 e^2 \left(2 - 5\frac{a_0^2}{r_0^2} \cos^2(\lambda_0 - \varpi)\right) \\ &= -\left(\frac{\mu^2}{2\Lambda^2} - \frac{Gm_0 \Lambda^4}{4r_0^3 \mu^2}\right) \\ &\quad - \frac{3Gm_0}{8a_0^3} \frac{\Lambda^4}{\mu^2} \left(1 - \left(1 - \frac{D}{\Lambda}\right)^2\right) (5 \cos(2(\lambda_0 - \varpi)) + 1) \end{aligned} \quad (17)$$

where the semicolon symbol is used to separate the coordinates and their conjugated momenta.

Noticing that  $\dot{\Lambda} = -\frac{\partial H}{\partial \lambda} = 0$ , another degree of freedom  $(\Lambda; \lambda)$  is also removed and the terms depending exclusively on  $\Lambda$  can be dropped out. Since a Hamiltonian is defined to be autonomous if it doesn't depend explicitly on time, the Hamiltonian 17 is indeed a one-degree-of-freedom non-autonomous Hamiltonian  $H(D; -\varpi, t)$ , depending on time via the mean longitude  $\lambda_0$ .

### 2.1.3 Autonomous one-parameter dimensionless Hamiltonian

To make the Hamiltonian autonomous, the time dependency implied in the mean longitude of the perturbator  $\lambda_0$  should be removed, where  $\lambda_0$  is defined by the product of its mean motion  $n_0 = \sqrt{G(m_0 + m_p)/a_0^3}$  and time,  $\lambda_0 = n_0 t$ . It can be done by going into the extended phase space, through adding another degree of freedom  $(\Lambda_0; \lambda_0)$  without changing the solutions:

$$H(D, \Lambda_0; -\varpi, \lambda_0) = -\frac{3Gm_0}{8a_0^3} \frac{\Lambda^4}{\mu^2} \left(1 - \left(1 - \frac{D}{\Lambda}\right)^2\right) (5 \cos(2(\lambda_0 - \varpi)) + 1) + n_0 \Lambda_0 \quad (18)$$

To remove again this fake degree of freedom that I added artificially, I will look for a canonical transformation that makes one of the conjugate variables become  $(\lambda_0 - \varpi)$ . Assuming that the transformation takes the form  $(D, \Lambda_0; -\varpi, \lambda_0) \rightarrow (\Sigma_1, \Sigma_2; \sigma, \sigma_2)$ , the matrix  ${}^t \mathcal{A}^{-1}$  in the canonicity criterion 15 is

$$\begin{cases} \sigma = \lambda_0 - \varpi \\ \sigma_2 = \lambda_0 \end{cases} \Rightarrow {}^t \mathcal{A}^{-1} = \begin{pmatrix} 1 & 1 \\ 0 & 1 \end{pmatrix} \quad (19)$$

The matrix  $\mathcal{A}$  can be computed from  ${}^t \mathcal{A}^{-1}$ ,

$$\mathcal{A} = \begin{pmatrix} 1 & 0 \\ -1 & 0 \end{pmatrix} \Rightarrow \begin{cases} \Sigma_1 = D \\ \Sigma_2 = \Lambda_0 - D \end{cases} \quad (20)$$



and the Hamiltonian becomes

$$\begin{aligned} H(D, \Sigma_2; \sigma, \lambda_0) &= H(D, \Lambda_0 - D; \lambda_0 - \varpi, \lambda_0) \\ &= n_0(\Sigma_2 + D) - \frac{3Gm_0}{8a_0^3} \frac{\Lambda^4}{\mu^2} \left(1 - \left(1 - \frac{D}{\Lambda}\right)^2\right) (5 \cos(2\sigma) + 1) \end{aligned} \quad (21)$$

It's no longer explicitly dependent of  $\lambda_0$ , then  $\Sigma_2$  is actually a constant because of  $\dot{\Sigma}_2 = -\frac{\partial H}{\partial \lambda_0} = 0$ . After rearranging the terms, I finally get the one-degree-of-freedom autonomous Hamiltonian

$$\begin{aligned} H(D; \sigma) &= D \left[ n_0 - \frac{3n_0^2}{8n} \left(2 - \frac{D}{\Lambda}\right) (5 \cos(2\sigma) + 1) \right] \\ &= \left(n_0 - \frac{3n_0^2}{4n}\right) D + \frac{3n_0^2}{n} \frac{D^2}{\sqrt{\mu a}} - \frac{15n_0^2}{4n} D \cos 2\sigma + \mathcal{O}(D^2 \cos 2\sigma) \\ &\simeq \alpha D + \beta \frac{D^2}{\sqrt{\mu a}} - \gamma D \cos 2\sigma \end{aligned} \quad (22)$$

$$\text{with } \begin{cases} \alpha = n_0 - \frac{3n_0^2}{4n} \\ \beta = \frac{3n_0^2}{n} \\ \gamma = \frac{15n_0^2}{4n} \end{cases}$$

The tidal bulge on the planet can be included in the model by adding a potential term to the Hamiltonian [1]

$$V_{\text{bulge}} = -\frac{Gm_p R_p^2}{2r^5} J_2 \left[r^2 - 3(\hat{\mathbf{k}} \cdot \mathbf{r})^2\right] \quad (23)$$

where  $J_2 = \frac{1}{2} \frac{\Omega_p^2 R_p^3}{GM_p}$  is the oblateness of the planet.

I compute the averaged potential before adding this term into the averaged Hamiltonian, assuming that the orbit of the particle is in the  $xy$  plane ( $\hat{\mathbf{k}} \cdot \mathbf{r} = 0$ )

$$\begin{aligned} \overline{V_{\text{bulge}}} &= \frac{1}{2\pi} \int_0^{2\pi} V_{\text{bulge}} dM = -\frac{Gm_p J_2 R_p^2}{4\pi} \int_0^{2\pi} \frac{1}{r^3} dM \\ &= -\frac{Gm_p J_2 R_p^2}{2} \left(\frac{1}{a^3 (1 - e^2)^{\frac{3}{2}}}\right) \\ &= -\frac{n\Lambda J_2 R_p^2}{2a^2 (1 - e^2)^{\frac{3}{2}}} \end{aligned} \quad (24)$$

where  $Gm_p/a = \mu/a = \sqrt{\mu/a^3} \sqrt{\mu a} = n\Lambda$ .



With  $(1-e^2)^{1/2} = 1-D/\Lambda$ , I expand the last term for small eccentricities:  $(1-x^2)^{-3} = 1 + 3x + 6x^2 + \mathcal{O}(x^3)$  and get

$$\begin{aligned}\overline{V_{\text{bulge}}} &= -\frac{n\Lambda J_2 R_p^2}{2a^2} \left(1 - \frac{D}{\Lambda}\right)^{-3} \\ &= -\frac{n\Lambda J_2 R_p^2}{2a^2} \left(1 + \frac{3D}{\Lambda} + \frac{6D^2}{\Lambda^2} + \mathcal{O}(D^3)\right) \\ &= -\frac{n\Lambda J_2 R_p^2}{2a^2} - \frac{3nJ_2 R_p^2}{2a^2} D - \frac{3nJ_2 R_p^2}{a^2} \frac{D^2}{\Lambda} + \mathcal{O}(D^3)\end{aligned}\quad (25)$$

where the first term is a constant that can be simply dropped out.

The Hamiltonian with the tidal bulge included in the model is thus

$$\begin{aligned}H(D; \sigma) &= D \left[ n_0 - \frac{3n_0^2}{8n} \left(2 - \frac{D}{\Lambda}\right) (5 \cos(2\sigma) + 1) \right] - \frac{n\Lambda J_2 R_p^2}{2a^2(1-e^2)^{\frac{3}{2}}} \\ &= \left( n_0 - \frac{3n_0^2}{4n} - \frac{3}{2}nJ_2 \frac{R_p^2}{a^2} \right) D + \left( \frac{3n_0^2}{n} - 3nJ_2 \frac{R_p^2}{a^2} \right) \frac{D^2}{\sqrt{\mu a}} - \left( \frac{15n_0^2}{4n} \right) D \cos 2\sigma \\ &\quad + \mathcal{O}(D^2 \cos 2\sigma) + \mathcal{O}(D^3) \\ &\simeq \alpha D + \beta \frac{D^2}{\sqrt{\mu a}} - \gamma D \cos 2\sigma\end{aligned}$$

which takes the same form as the Hamiltonian 22, but with  $J_2$  included in the definitions of  $\alpha$  and  $\beta$

$$\begin{cases} \alpha = n_0 - \frac{3n_0^2}{4n} - \frac{3}{2}nJ_2 \frac{R_p^2}{a^2} \\ \beta = \frac{3n_0^2}{n} - 3nJ_2 \frac{R_p^2}{a^2} \\ \gamma = \frac{15n_0^2}{4n} \end{cases} \quad (26)$$

A q-order resonance takes the general form:  $H^q = \alpha\Sigma + \beta\Sigma^2 + \gamma\Sigma^{\frac{q}{2}} \cos q\sigma$ . By ignoring higher orders, the Hamiltonian of the hierarchical restricted 3-body problem  $H(D; \sigma)$  is indeed a 2<sup>nd</sup> order resonance, with the resonance angle  $\sigma = \lambda_0 - \varpi$ .

Notice that  $\beta = \frac{3n_0^2}{n} - 3nJ_2 \frac{R_p^2}{a^2} \begin{cases} < 0 \text{ for small } a \\ > 0 \text{ for large } a \end{cases}$ , as the tidal bulge term becomes negligible at large semi-major axes. By doing another transformation, I get

$$\begin{cases} H' = \frac{H}{\sqrt{\mu a}} \\ \Sigma = \frac{D}{\sqrt{\mu a}} \end{cases} \Rightarrow H'(\Sigma; \sigma) = \alpha\Sigma \mp |\beta|\Sigma^2 - \gamma\Sigma \cos 2\sigma \begin{cases} - \text{ for small } a \\ + \text{ for large } a \end{cases} \quad (27)$$

This transformation is not canonical. But the variables can still be treated as canonical because the equations of motion preserve the Hamiltonian structure:

$$\begin{cases} \dot{\Sigma} = \frac{\dot{D}}{\sqrt{\mu a}} = -\frac{1}{\sqrt{\mu a}} \frac{\partial H}{\partial \sigma} = -\frac{\partial H'}{\partial \sigma} \\ \dot{\sigma} = \frac{\partial H}{\partial D} = \sqrt{\mu a} \frac{\partial H'}{\partial \Sigma} = \frac{\partial H'}{\partial \Sigma} \end{cases} \quad (28)$$

Both  $\Sigma$  and  $\sigma$  become dimensionless and  $H'$  has a dimension of frequency. In order to obtain an one-parameter dimensionless Hamiltonian, I perform another non-canonical transformation, which can be considered canonical for the same reason above:

$$\begin{cases} H'' = \frac{H'}{\omega} \\ \Phi = \frac{\Sigma}{k} \\ \phi = \sigma \end{cases} \Rightarrow H''(\Phi; \phi) = \frac{\alpha k}{\omega} \Phi \mp \frac{|\beta| k^2}{\omega} \Phi^2 - \frac{\gamma k}{\omega} \Phi \cos 2\phi \begin{cases} - \text{ for small } a \\ + \text{ for large } a \end{cases} \quad (29)$$

By choosing  $k, \omega$  such that the Hamiltonian takes the form  $H(\Phi; \phi) = \delta \Phi \mp \Phi^2 - \Phi \cos 2\phi$ , I get the expression for  $\delta$ :

$$\begin{cases} \frac{\alpha k}{\omega} = \delta \\ \frac{|\beta| k^2}{\omega} = 1 \\ \frac{\gamma k}{\omega} = 1 \end{cases} \Rightarrow \begin{cases} k = \frac{\gamma}{|\beta|} \\ \omega = \gamma k = \frac{\gamma^2}{|\beta|} \\ \delta = \frac{\alpha k}{\omega} = \frac{\alpha}{\gamma} \end{cases} \quad (30)$$

It's surprising that  $\delta$  is independent of  $|\beta|$ . It actually depends on  $a, n, J_2$ :

$$\delta(a, n, J_2) = \delta(a) = \frac{1}{5} \left( \frac{4}{3} \frac{n}{n_0} - 2J_2 \frac{n^2 R_p^2}{n_0^2 a^2} - 1 \right) \quad (31)$$

$$\text{with } \begin{cases} n(a) = \sqrt{\frac{\mu}{a^3}} \\ J_2(a) = \frac{1}{2} \frac{\Omega_p^2(a) R_p^3}{G m_p} \\ \Omega_p(a) = \frac{L_0 - m \sqrt{\mu a (1 - e^2)}}{I_p m_p R_p^2} \end{cases}$$

where  $\Omega_p$  is the rotational velocity of the planet,  $L_0$  is the total angular momentum in the planet-satellite system,  $I_p$  is the moment of inertia of the planet.

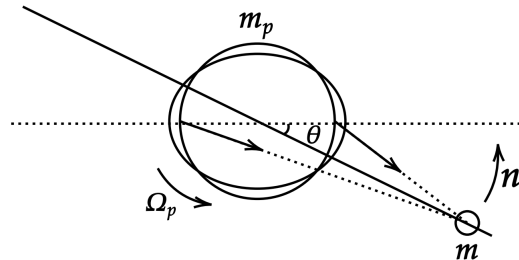


Figure 4: Schema of the tidal interaction in a planet-satellite system ( $\Omega_p > n$ )

The tidal effect leads to the variation of the semi-major axes in a prograde orbit where the satellite orbits the planet in the same direction as the latter rotates on itself, as shown



in the figure 4. If the rotational velocity of the planet  $\Omega_p$  exceeds the orbital velocity of the satellite  $n$ , the tidal bulges are misaligned with respect to the planet-satellite direction  $\mathbf{r}$  by an angle  $\theta = (\Omega_p - n)\Delta t$ , where  $\Delta t$  is the constant time lag measuring the tidal dissipation [7]. The torque exerted on the bulges slows down the rotation of the planet, and the orbit of the satellite expands as a result of the conservation of total angular momentum. If  $\Omega_p < n$ , the planet rotates faster and the orbit of the satellite migrates inward.

It can be noticed that the parameter  $\delta$ , which determines the topology of the phase space, is varying only with the semi-major axes. As the satellite gets away from the planet due to the tidal effect, certain ranges of  $\delta$  allows the occurrence of the evection resonance, as will be explained in the next section. From this property, the history of  $\delta$  is easily traced in the section 2.2.2.

## 2.2 Analysis of the phase space $H(\Phi; \phi)$

### 2.2.1 Bifurcations of topology of the phase space

The one-degree-of-freedom autonomous Hamiltonian of the hierarchical restricted 3-body problem has been simplified to be

$$H(\Phi; \phi) = \delta\Phi \mp \Phi^2 - \Phi \cos 2\phi \begin{cases} - \text{ for small } a \\ + \text{ for large } a \end{cases} \quad (32)$$

where  $\begin{cases} \Phi = \frac{|\beta|}{\gamma} (1 - \sqrt{1 - e^2}) \approx \frac{|\beta|}{2\gamma} \text{ for small eccentricities} \\ \phi = \lambda_0 - \varpi, \text{ which is the resonance angle} \end{cases}$

I recall that  $\lambda_0 = n_0 t$  is the mean longitude of the perturbator, and  $\varpi = \omega + \Omega$  is the longitude of periapsis of the particle.

Let  $\begin{cases} X = \sqrt{2\Phi} \cos \phi \\ Y = \sqrt{2\Phi} \sin \phi \end{cases}$ ,  $H(\Phi; \phi)$  can be written as

$$H(X, Y) = \frac{\delta}{2} (X^2 + Y^2) \mp \frac{1}{4} (X^2 + Y^2)^2 - \frac{1}{2} (X^2 - Y^2) \quad (33)$$

The transformation  $(\Phi, \phi) \rightarrow (X, Y)$  is proven to be canonical in the Appendix B. By equating the right-hand-side of the equations of motion to 0 and solving

$$\begin{cases} \dot{X} = -\frac{\partial H}{\partial Y} = 0 \\ \dot{Y} = \frac{\partial H}{\partial X} = 0 \end{cases} \quad (34)$$

the number of solutions corresponds to the number of fixed points in the phase space. While the number of fixed points changes, the bifurcations occur and the topology of the phase space changes.

1. At small semi-major axes, the equations 34 are  $\begin{cases} X(X^2 + Y^2 - \delta + 1) = 0 \\ Y(X^2 + Y^2 - \delta - 1) = 0 \end{cases}$ , and the solutions are given in the table 1 below.

Small a	$\delta < -1$	$-1 < \delta < 1$	$\delta > 1$
Number of solutions	1	3	5
Fixed points	$(0, 0)$	$(0, 0), (0, \pm\sqrt{\delta+1})$	$(0, 0), (0, \pm\sqrt{\delta+1}), (\pm\sqrt{\delta-1}, 0)$

Table 1: Fixed points at small semi-major axis

2. At large semi-major axis, the equations 34 are  $\begin{cases} X(X^2 + Y^2 + \delta - 1) = 0 \\ Y(X^2 + Y^2 + \delta + 1) = 0 \end{cases}$ , and the solutions are given in the table 2 below.

Large a	$\delta < -1$	$-1 < \delta < 1$	$\delta > 1$
Number of solutions	5	3	1
Fixed points	$(0, 0), (\pm\sqrt{1-\delta}, 0), (0, \pm\sqrt{-\delta-1})$	$(0, 0), (\pm\sqrt{1-\delta}, 0)$	$(0, 0)$

Table 2: Fixed points at large semi-major axis

Taking the evection resonance at small semi-major axes in the Sun-Earth-Moon system as an example, the bifurcations are shown in the figure 5. There are mainly three configurations of the topology of the phase space:

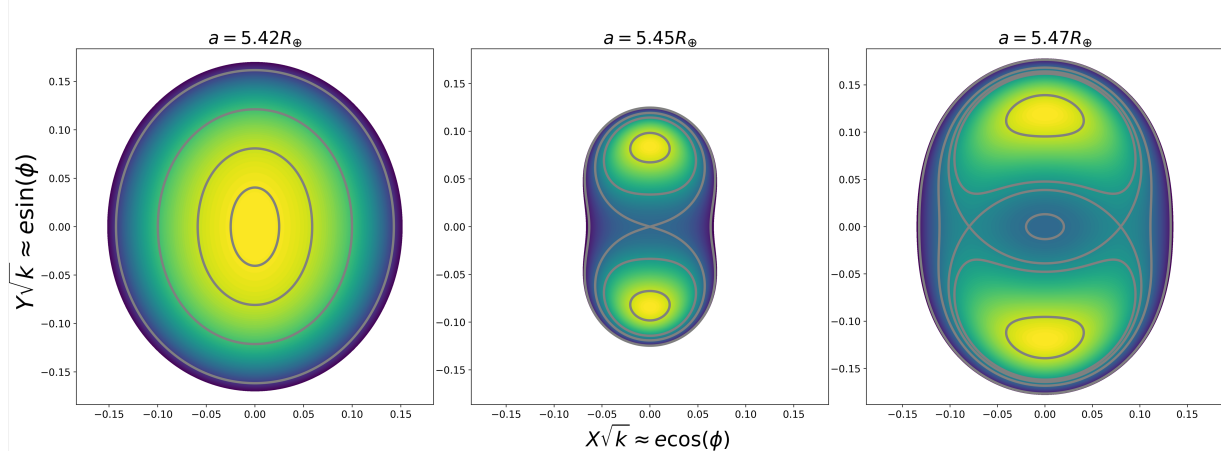


Figure 5: Phase space  $H(\Phi, \phi) = H(X, Y)$  of the Sun-Earth-Moon system

- $\delta < -1$  ( $a = 5.42R_\oplus$  in the example): There is only one fixed point in the center where  $e = 0$ , which means that the satellite has a very stable circular orbit around the fixed point.
- $-1 < \delta < 1$  ( $a = 5.45R_\oplus$  in the example): There are three fixed points, with one in the center and the other two respectively above and below. There's no more stable

orbits in the center since the fixed point  $(0, 0)$  has become an unstable one. The satellite is captured by an orbit around one of the two stable fixed points at large eccentricities, and the resonance angle  $\phi$  will oscillate around  $\pi/2$  (for the fixed point above) or  $3\pi/2$  (for the one below) instead of circulating from 0 to  $2\pi$ . It indicates that  $(\lambda_0 - \varpi)$  is a constant and the satellite's orbit is precessing as fast as the variation of the mean longitude of the star. This bifurcation from 1 to 3 fixed points marks that the system has entered into the evection resonance.

- $\delta > 1$  ( $a = 5.47R_\oplus$  in the example): There are in total five fixed points, with two more on the left and right compared to the previous case. A new stable zone is allowed in the center, however the satellite won't get back immediately to a stable orbit. It stays around one of the fixed points above and below, and will eventually be recaptured by the central zone as the zone enlarges while the semi-major axes increases. Thus, the evection resonance won't end as the second bifurcation (from 3 to 5 fixed points) occurs. As the resonant libration amplitude increases, the resonance angle circulates again when the satellite gets back to a stable circular orbit in the center [8].

Two evection resonances are expected from solving the equations of motion, separately at small and large semi-major axes. However, it is still necessary to study precisely whether the parameter  $\delta$  will actually reach twice the values indicating the beginning of the evection resonance, as what I'll do for the next section.

### 2.2.2 History of the parameter $\delta$ and the two evection resonances

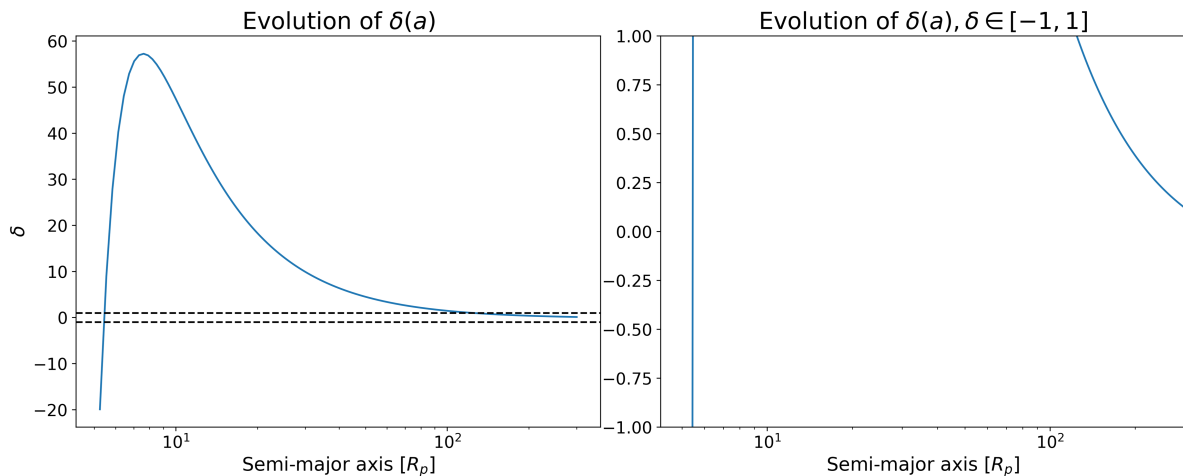


Figure 6:  $\delta(a)$  history of the Sun-Earth-Moon system

From the equation 31 I know that the only parameter which appears in the simplified Hamiltonian just has one variable: the semi-major axes. It would be very helpful to trace the variation of  $\delta$  as a function of  $a$  to find out when and how many times a system is



going to experience the evection resonance. Following the same equation, the evolution of  $\delta(a)$  is plotted in the figure 6.

The tidal bulge on the planet dominates for very close-in orbits and is negligible only for faraway orbits. The figure 6 confirms that the system will enter into the first evection resonance by increasing from below -1 to over 1. Then the satellite is recaptured by a stable orbit at some time when  $\delta > 1$ . As the satellite spirals away,  $\delta$  goes below 1, the system enters the second evection resonance and stays there until it completely gets out of the system, since it requires a negative mean motion  $n$  to let  $\delta$  reach -1 if  $J_2$  is ignored.

Therefore, for a satellite which is initially at a very close-in orbit and which gradually moves away by gaining angular momentum from the planet, it can be summarized as in the figure 7 that:

- The first evection resonance takes place when  $\delta$  rises up to -1 at small semi-major axes. Then it quickly evolves to 1 and stable circular orbits are allowed again. This resonance ends at some time during  $\delta > 1$ , as the satellite is recaptured by the enlarging stable zone in the center of the phase space.
- The second evection resonance occurs when  $\delta$  drops down to 1 at large semi-major axes. Since the oblateness of the planet  $J_2$  can be ignored for faraway orbits, this condition yields

$$\delta = \frac{1}{5} \left( \frac{4}{3} \frac{n}{n_0} - 1 \right) = 1 \Rightarrow \frac{n}{n_0} = \frac{9}{2} \quad (35)$$

By replacing the mean motions of the particle and of the perturbator with the expressions derived from the Kepler's Third Law:  $n = \sqrt{Gm_p/a^3}$ ,  $n_0 = \sqrt{Gm_0/a_0^3}$ , the position of the second evection resonance is

$$a_{\text{2nd ER}} = \left( \frac{4m_p}{81m_0} \right)^{1/3} a_0 \quad (36)$$

I notice that the mass ratio term can be replaced by introducing the Hill radius  $R_{\text{Hill}} = a_0 (m_p/3m_0)^{\frac{1}{3}}$ , which is the boundary at which the planet's gravitational pull on the particle is equal to that of the perturbator.

$$a_{\text{2nd ER}} = \left( \frac{4m_p}{81m_0} \frac{3m_0}{m_p} \right)^{\frac{1}{3}} R_{\text{Hill}} = \left( \frac{4}{27} \right)^{\frac{1}{3}} R_{\text{Hill}} \approx 0.529 R_{\text{Hill}} \quad (37)$$

The parameter  $\delta$  then remains between -1 and 1 for the rest of the life of the 3-body system, and never reaches again -1, which means that no stable zone is allowed anymore in the center of the phase space. The profile of the phase space is rotated by  $\pi/2$  compared to the first evection resonance, thus the resonance angle will oscillate around 0 or  $\pi$ .

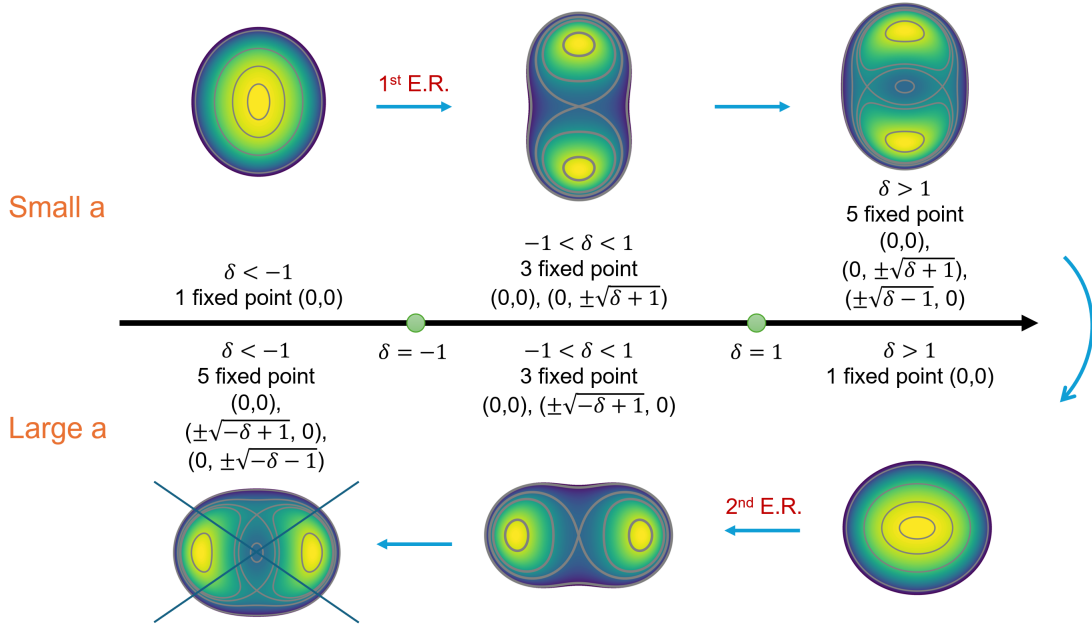


Figure 7: The evolution of topology of the phase space in the hierarchical restricted 3BP

### 3 Numerical simulations

NcorpiON is a sophisticated software designed for N-body problem simulations, especially for planetary systems [1]. Advanced algorithms are implemented to handle the mutual gravity among multiple objects as well as their tidal interactions. The advantage compared to the previous N-body simulation integrators is that NcorpiON takes into account the fragmentation as an important outcome of the system. By simply adjusting the parameters of the particles, all the information about the orbits during the simulation as well as a 3D real-time visualization are available.

By using NcorpiON, I simulated the Sun-Earth-Moon system soon after the moon's formation and a selected exoplanetary system near the Hill sphere. It is because the former would never experience the second ejection resonance due to the lack of angular momentum in the Earth-Moon 2-body system, while the latter cannot have passed through the first ejection resonance which would have occurred inside the Roche radius, as will be explained in detail in the sections 3.1.1 and 3.2.

#### 3.1 Simulation for the Sun-Earth-Moon system

From the analytical part, theoretical values of the critical semi-major axes for the ejection resonance can be obtained by looking for the bifurcations of topology in the phase space.

- $a_1 \approx 5.43R_{\oplus}$  where the first ejection resonance occurs;
- $a_2 \approx 124.3R_{\oplus}$  where the second ejection resonance occurs.

### 3.1.1 Searching for the second evection resonance in the future

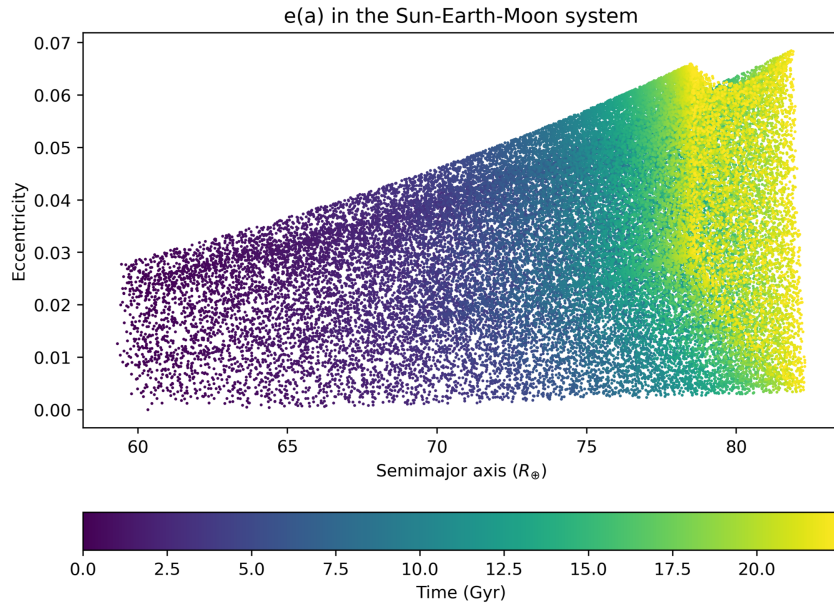


Figure 8: Searching for the second evection resonance of the Sun-Earth-Moon system

The second evection resonance would take place at  $a_2 = 124.3R_\oplus$  theoretically, however it never shows up in the simulation starting from the current orbit  $a_{\text{current}} = 60.3R_\oplus$ , even if NcorpiON is run for longer periods of time. The reason is that the Earth-Moon system doesn't have enough angular momentum to allow the moon to reach  $a_2$ . Currently the Earth is rotating slightly quicker than the moon's orbital velocity, and is actually spinning down due to the torque exerted on the tidal bulge. The moon is thus migrating outward and will reach  $86R_\oplus$  at maximum before being tidally locked to the Earth, which marks the end of the dynamical evolution of the system. The moon is simply not able to get far enough to get into the second evection resonance.

### 3.1.2 Searching for the first evection resonance in the past

Assuming the moon was formed from a giant impact and stayed in an orbit at  $a \approx 4R_\oplus$  at the beginning, it would have entered into the first evection resonance very rapidly. The variation of the resonance angle  $\phi$ , the eccentricity of the moon's orbit and the total angular momentum in the Earth-Moon system as a function of the semi-major axes are shown in the figures 9, 10 below.

The first evection resonance occurs exactly where I expected it to be. The eccentricity of the orbit has increased rather fast and even reached 0.6: It's clear that the moon has been captured during the simulation by the fixed point on the bottom in the figure 5, since the resonance angle is oscillating around  $3\pi/2$  and that the orbits far from the center of the phase space are highly eccentric, as explained in the section 2.2.1.

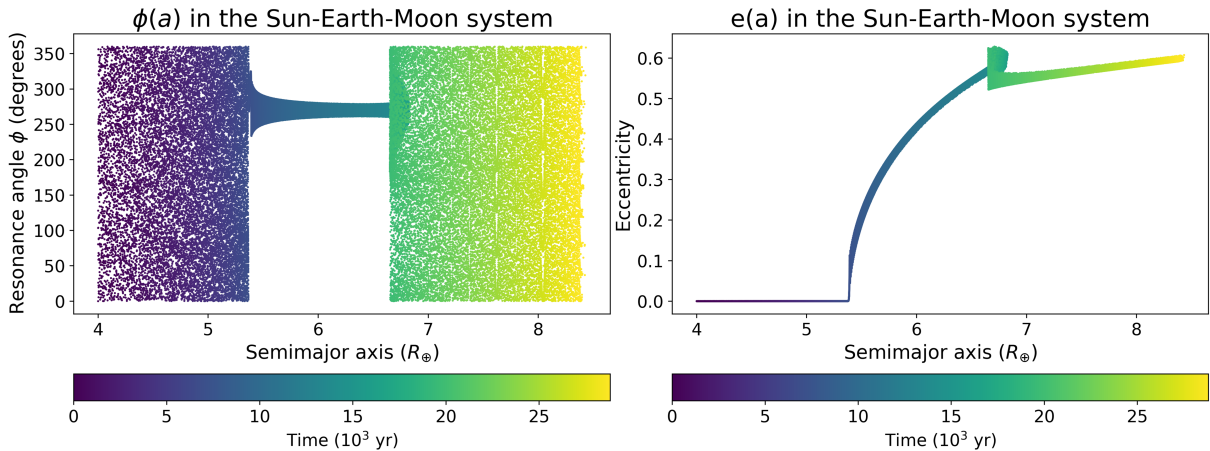
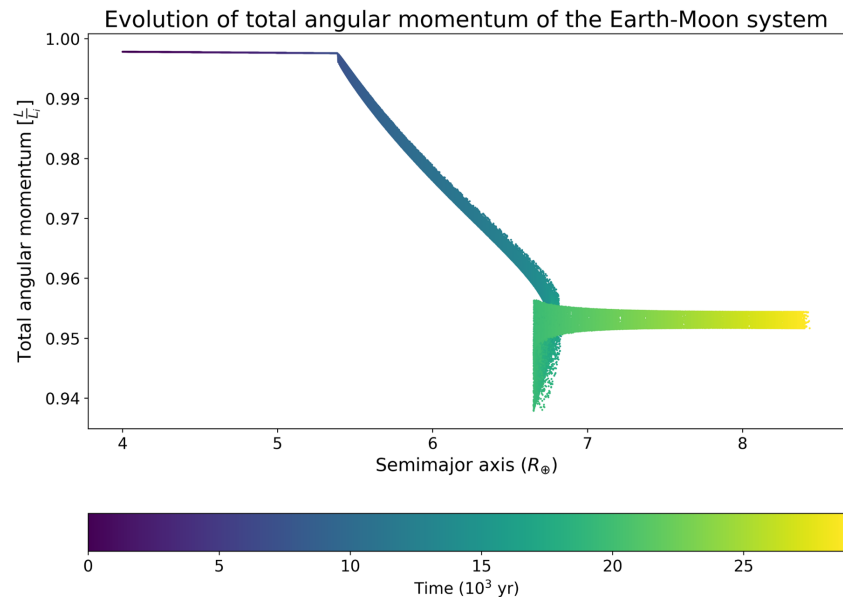

 Figure 9: Resonance angle  $\phi$  and eccentricity of moon's orbit during the first resonance


Figure 10: Angular momentum of the Earth-Moon system during the first resonance

Around 5% of the total angular momentum in the Earth-Moon system that has been lost is indeed transferred to the Sun-Earth system, indicating a chain of angular momentum transfer during the resonance, from the Earth's spin to the moon's orbit and eventually to the Earth's orbit [9, 10, 11]. A slightly backward evolution at the end of the resonance has also been noticed, because the satellite is moving much faster at the periapsis in a highly eccentric orbit due to the Kepler's second law. Its orbital velocity can be even faster than the rotational velocity of the planet, letting the tidal effect transfer angular momentum from the satellite's orbit back to the spin of the planet and causing the orbit to shrink.



## 3.2 Simulation for the exoplanetary system of TOI-6303 b

### 3.2.1 Selection of the planet

Since there's no method up to now to detect exomoons, no real exoplanetary system is available to study the problem of interest. However, it could be interesting to pick up an exoplanet that would allow me to see the second evection resonance by simulation. The parameters of exoplanets should be carefully checked so that an exomoon is possible and probable to exist at least for a relatively long period of time. More specifically, the planet should have a large safe zone for the satellite to live in, defined as the region between the Roche radius and the Hill radius.

- The Roche radius  $R_{\text{Roche}} = 2.44R_p (\rho_p/\rho)^{1/3}$  is the minimal semi-major axes of the satellite's orbit so that it won't be torn apart by the tidal forces of the planet [12].
- The Hill radius  $R_{\text{Hill}} = a_0 (m_p/3m_0)^{1/3}$  is defined as the maximal semi-major axes within which the gravity of the planet dominates.

I set the selection criteria to be  $R_{\text{Hill}}/R_{\text{Roche}} \approx 10$ , and by searching among the detected exoplanets, TOI-6303 b seems to be a good choice [13]. Basic information regarding this planet and its star are given below.

$m_0$	$R_0$	$m_p$	$R_p$	a	Orbital period of the planet
$0.64M_\odot$	$0.61R_\odot$	$7.84M_J$	$1.03R_J$	0.076 AU	9.49 days

Table 3: Information on TOI-6303 b system

When artificially setting up a satellite, several conditions have to be met.

- The planet should not rotate too fast to disintegrate. Its rotational velocity is required to satisfy  $\Omega_p \ll \sqrt{GM_p/R_p^3}$ .
- The planet should not rotate too slowly to avoid getting into the same situation as the Sun-Earth-Moon system: The total angular momentum is not enough to let the satellite evolve until the second evection resonance.
- The satellite has an appropriate mass and density:  $m \approx M_p/1000$ ,  $\rho = \rho_p$ .
- The rotational velocity of the planet has to be higher than the orbital velocity of the satellite ( $\Omega_p > n$ ) so that the angular momentum is transferred in the correct direction and that the satellite actually moves outward.

The set-up values of the artificial satellite as well as the Roche radius and the Hill radius are listed in the table 4.

$m$	$25M_{\oplus}$
$R$	$1.16R_{\oplus}$
Rotational period of the planet	11.1 hours
Orbital period of the satellite	25.1 hours
$R_{\text{Roche}}$	$2.44R_p$
$R_{\text{Hill}}$	$24.3R_p$
Maximal semi-major axes	$1288R_p$

Table 4: Set-up values on the TOI-6303 b system

### 3.2.2 Searching for second evection resonance

By analyzing the phase space of the TOI-6303 b system, the two evection resonances should ideally occur at  $a_1 = 1.153R_p$  and  $a_2 = 12.785R_p$ . Since  $a_1 < R_{\text{Roche}}$ , the satellite wouldn't have lived in the orbit where the system enters the first evection resonance. I launched the simulation with the satellite which is initially at  $7.5R_p$  and the second evection resonance appears in the figures below.

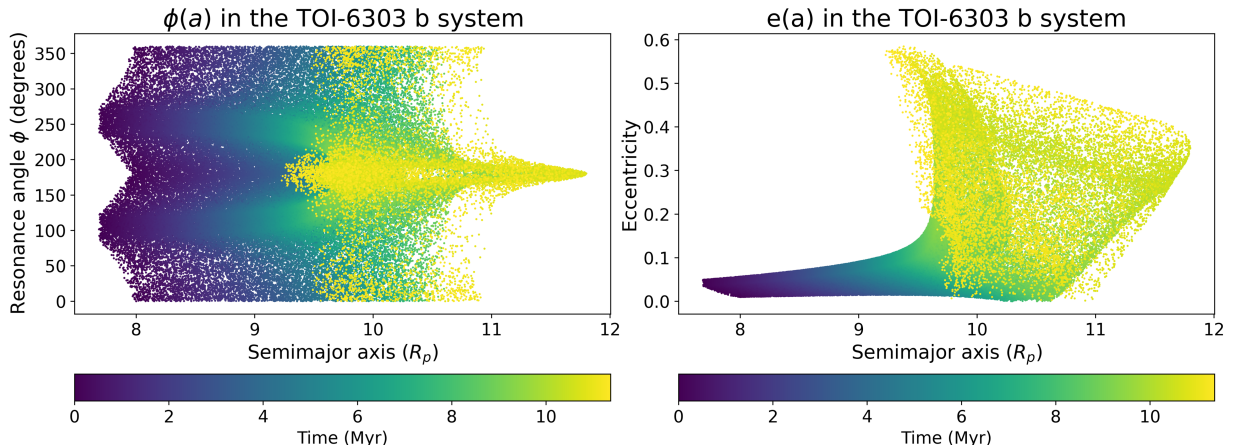


Figure 11: The second evection resonance in the TOI-6303 b system

The resonance angle oscillates around  $\pi$ , since the two fixed points other than  $(0, 0)$  are on the  $x$ -axis for the second evection resonance. It could also be noticed that the figure 11 doesn't look exactly the same as the figure 9 for the Sun-Earth-Moon system, and the system enters the resonance at around  $a = 10R_p$ , well before the prediction. It is because the simulation becomes less accurate for orbits near the Hill sphere, i.e. for the second resonance compared to the first one, due to the assumptions that I made. The chaotic nature of orbits near the Hill radius introduces great limitations to the precision of the simulation: higher-order terms in the equation 7 cannot be ignored anymore, the gravitational influence of the star is no longer small enough for us to apply the perturbation theory.



## 4 Conclusion

In this project, I firstly derived the mathematical description of the evection resonance, which is by definition a second-order resonance between the mean longitude of the star and the longitude of periapsis of the satellite. The Hamiltonian is simplified to be

$$H(\Phi; \phi) = \delta\Phi \mp \Phi^2 - \Phi \cos 2\phi \begin{cases} - & \text{for small } a \\ + & \text{for large } a \end{cases}$$

A hierarchical restricted 3-body problem where the satellite migrates outward due to the tidal interaction will undergo twice the evection resonance respectively in a close-in and faraway orbit, during which the eccentricity of the satellite's orbit is greatly excited. The system gets out of the resonance in between the two, but would stay in the second one until the end of the system. Thanks to NcorpiON software and the Bonsai cluster of the University, I've also gained experience in simulating 3-body problems to confirm the theoretical results. In fact, some of the systems, such as ours, don't even have the opportunity to go through the second evection resonance because of the lack of the available angular momentum.

The evection resonance helps also to understand the orbital evolution of the satellite, as well as other phenomena appearing in the history of the planet-satellite system, for instance the loss of total angular momentum of the planet-satellite two-body system. The same analysis could be done for other satellites in the solar systems as well to check whether one or both resonances are possible to happen, and if we detect exomoons one day, the evolution of their orbits could be better predicted by incorporating the evection resonance theory.



## References

- [1] Jérémie Couturier, Alice C. Quillen, and Miki Nakajima. “NcorpiON : A  $O(N)$  software for N-body integration in collisional and fragmenting systems”. In: *New Astronomy* 114 (Jan. 1, 2025), p. 102313. ISSN: 1384-1076. DOI: [10.1016/j.newast.2024.102313](https://doi.org/10.1016/j.newast.2024.102313).
- [2] G. Boué and J. Laskar. “Precession of a planet with a satellite”. In: *Icarus* 185.2 (Dec. 1, 2006), pp. 312–330. ISSN: 0019-1035. DOI: [10.1016/j.icarus.2006.07.019](https://doi.org/10.1016/j.icarus.2006.07.019). (Visited on 01/08/2025).
- [3] Antoine Petit. “Architecture and stability of planetary systems”. PhD thesis. Université Paris sciences et lettres, June 28, 2019.
- [4] Jérémie Couturier. “Lidov-Kozai mechanism and evection resonance”. In: () .
- [5] Jérémie Couturier. “Dynamics of co-orbital planets. Tides and resonance chains”. PhD thesis. Observatoire de Paris, Oct. 21, 2022.
- [6] Jacques Laskar. “Andoyer construction for Hill and Delaunay variables”. In: *Celestial Mechanics and Dynamical Astronomy* 128.4 (Aug. 1, 2017), pp. 475–482. ISSN: 1572-9478. DOI: [10.1007/s10569-017-9761-0](https://doi.org/10.1007/s10569-017-9761-0). (Visited on 01/08/2025).
- [7] P. Hut. “Tidal evolution in close binary systems.” In: *Astronomy and Astrophysics* 99 (June 1, 1981). ADS Bibcode: 1981A&A....99..126H, pp. 126–140. ISSN: 0004-6361. (Visited on 01/09/2025).
- [8] Matija Ćuk and Sarah T. Stewart. “Making the Moon from a Fast-Spinning Earth: A Giant Impact Followed by Resonant Despinning”. In: *Science* 338.6110 (Nov. 23, 2012). Publisher: American Association for the Advancement of Science, pp. 1047–1052. DOI: [10.1126/science.1225542](https://doi.org/10.1126/science.1225542).
- [9] Jihad Touma and Jack Wisdom. “Resonances in the Early Evolution of the Earth-Moon System”. In: *The Astronomical Journal* 115.4 (Apr. 1, 1998). Publisher: IOP Publishing, p. 1653. ISSN: 1538-3881. DOI: [10.1086/300312](https://doi.org/10.1086/300312).
- [10] R. Rufu and R. M. Canup. “Tidal Evolution of the Evection Resonance/Quasi-Resonance and the Angular Momentum of the Earth-Moon System”. In: *Journal of Geophysical Research: Planets* 125.8 (2020), e2019JE006312. ISSN: 2169-9100. DOI: [10.1029/2019JE006312](https://doi.org/10.1029/2019JE006312).
- [11] Kevin J. Zahnle et al. “The tethered Moon”. In: *Earth and Planetary Science Letters* 427 (Oct. 2015), pp. 74–82. ISSN: 0012821X. DOI: [10.1016/j.epsl.2015.06.058](https://doi.org/10.1016/j.epsl.2015.06.058). (Visited on 12/15/2024).
- [12] Valeri V. Makarov and Michael Efroimsky. “Pathways of survival for exomoons and inner exoplanets”. In: *Astronomy & Astrophysics* 672 (Apr. 2023), A78. ISSN: 0004-6361, 1432-0746. DOI: [10.1051/0004-6361/202245533](https://doi.org/10.1051/0004-6361/202245533). (Visited on 01/09/2025).
- [13] Andrew Hotnisky et al. *Searching for GEMS: Two Super-Jupiters around M-dwarfs – Signatures of Instability or Accretion?* Nov. 12, 2024. DOI: [10.48550/arXiv.2411.08159](https://doi.org/10.48550/arXiv.2411.08159). arXiv: [2411.08159\[astro-ph\]](https://arxiv.org/abs/2411.08159). (Visited on 12/15/2024).



## 5 Appendix

### 5.1 Appendix A: Canonicity of the Poincaré variables

For the transformation from the Delaunay variables  $(\Lambda, G, H; M, \omega, \Omega)$  to the Poincaré variables  $(\Lambda, D, Z; \lambda, -\varpi, -\Omega)$ , the non-degenerate matrix  ${}^t\mathcal{A}^{-1}$  in the canonicity criterion 15 reads

$$\begin{cases} \lambda = M + \omega + \Omega \\ -\varpi = \omega - \Omega \\ -\Omega = -\Omega \end{cases} \Rightarrow {}^t\mathcal{A}^{-1} = \begin{pmatrix} 1 & 1 & 1 \\ 0 & -1 & -1 \\ 0 & 0 & -1 \end{pmatrix} \quad (38)$$

The matrix  $\mathcal{A}$  can be computed from  ${}^t\mathcal{A}^{-1}$

$$\mathcal{A} = \begin{pmatrix} 1 & 0 & 0 \\ 1 & -1 & 0 \\ 0 & 1 & -1 \end{pmatrix}$$

I notice that the conjugated momenta of the Poincaré variables are indeed equal to the product of  $\mathcal{A}$  and the conjugated momenta of the Delaunay variables

$$\mathcal{A} \cdot \begin{pmatrix} \Lambda \\ G \\ H \end{pmatrix} = \begin{pmatrix} \Lambda \\ \Lambda - G \\ G - H \end{pmatrix} = \begin{pmatrix} \Lambda \\ D \\ Z \end{pmatrix} \quad (39)$$

and the canonicity of the Poincaré variables is thus assured by meeting the condition 15.

### 5.2 Appendix B: Canonicity of the transformation $(\Phi, \phi) \rightarrow (X, Y)$

A transformation is canonical if and only if its Jacobian is symplectic [5]. From the given transformation:

$$X = \sqrt{2\Phi} \cos \phi, \quad Y = \sqrt{2\Phi} \sin \phi$$

The Jacobian matrix of the transformation reads

$$J = \begin{bmatrix} \frac{\cos \phi}{\sqrt{2\Phi}} & -\sqrt{2\Phi} \sin \phi \\ \frac{\sin \phi}{\sqrt{2\Phi}} & \sqrt{2\Phi} \cos \phi \end{bmatrix} \quad (40)$$

with the determinant

$$\det(J) = \left( \frac{\cos \phi}{\sqrt{2\Phi}} \right) (\sqrt{2\Phi} \cos \phi) - \left( \frac{\sin \phi}{\sqrt{2\Phi}} \right) (-\sqrt{2\Phi} \sin \phi) = \cos^2 \phi + \sin^2 \phi = 1$$

The Poisson brackets in the  $(\Phi, \phi)$  coordinates are defined as:

$$\{f, g\} = \frac{\partial f}{\partial \Phi} \frac{\partial g}{\partial \phi} - \frac{\partial f}{\partial \phi} \frac{\partial g}{\partial \Phi}$$



Then the Poisson brackets for  $(X, Y)$  in terms of  $(\Phi, \phi)$ :

$$\begin{aligned}
 \{X, Y\} &= \frac{\partial X}{\partial \Phi} \frac{\partial Y}{\partial \phi} - \frac{\partial X}{\partial \phi} \frac{\partial Y}{\partial \Phi} \\
 &= \left( \frac{\cos \phi}{\sqrt{2\Phi}} \right) (\sqrt{2\Phi} \cos \phi) - (-\sqrt{2\Phi} \sin \phi) \left( \frac{\sin \phi}{\sqrt{2\Phi}} \right) \\
 &= \cos^2 \phi + \sin^2 \phi = 1 \\
 \{Y, X\} &= \{X, Y\} \\
 \{X, X\} &= \frac{\partial X}{\partial \Phi} \frac{\partial X}{\partial \phi} - \frac{\partial X}{\partial \phi} \frac{\partial X}{\partial \Phi} = 0 \\
 \{Y, Y\} &= \frac{\partial Y}{\partial \Phi} \frac{\partial Y}{\partial \phi} - \frac{\partial Y}{\partial \phi} \frac{\partial Y}{\partial \Phi} = 0
 \end{aligned} \tag{41}$$

verifies the invariance of Poisson brackets  $\{X, Y\} = \{Y, X\} = 1$ ,  $\{X, X\} = \{Y, Y\} = 0$ , which leads to the symplecticity of the Jacobian matrix. Therefore, the transformation  $(\Phi, \phi) \rightarrow (X, Y)$  is proved to be canonical.